

1 **Interpretive Summary**

2 **Strain hardening and anisotropy in tensile fracture properties of sheared model**

3 **Mozzarella cheeses. By Sharma et al.**

4 Mozzarella cheese has a fibrous appearance that is created during the working process  
5 involving kneading and stretching action. Energy imparted to the cheese during working  
6 determines its characteristics. The fibrous character of the cheese suggests the possibility of  
7 direction dependent (anisotropic) properties. This work investigates the effect of shear work  
8 input on strain hardening and anisotropy in the tensile properties. It also proposes schematic  
9 models to explain the observed anisotropy and strain hardening in sheared cheeses.

10 **Strain hardening and anisotropy in tensile fracture properties of sheared**  
11 **model Mozzarella cheeses**

12 **Prateek Sharma<sup>\*‡1</sup>, Peter A. Munro<sup>\*</sup>, Tzvetelin T. Dessev<sup>\*</sup>, Peter G. Wiles<sup>†</sup>, E. Allen**  
13 **Foegeding<sup>§</sup>**

14 *\*Riddet Institute, Massey University, Private Bag 11222, Palmerston North, New Zealand*

15 *†Fonterra Research and Development Centre, Private Bag 11029, Palmerston North 4442,*  
16 *New Zealand*

17 *‡Dairy Technology Division, National Dairy Research Institute, Karnal-132001, Haryana,*  
18 *India*

19 *§Department of Food, Bioprocessing and Nutrition Sciences, North Carolina State*  
20 *University, Box 7624, Raleigh, NC, 27695-7624, USA*

21

---

<sup>1</sup> Corresponding Author: Tel: +91 7082261083  
Email address: [P.Sharma@massey.ac.nz](mailto:P.Sharma@massey.ac.nz); [prateek.sharma@icar.gov.in](mailto:prateek.sharma@icar.gov.in);  
[prateeksharma2000@yahoo.com](mailto:prateeksharma2000@yahoo.com)

22

## ABSTRACT

23 We studied tensile fracture properties of model Mozzarella cheeses with varying amounts of  
24 shear work input (3.3-73.7 kJ/kg). After manufacture cheeses were elongated by manual  
25 rolling at 65 °C followed by tensile testing at 21 °C on dumbbell-shaped samples cut both  
26 parallel and perpendicular to the rolling direction. Strain hardening parameters were  
27 estimated from stress-strain curves using three different methods. Fracture stress and strain  
28 for longitudinal samples did not vary significantly with shear work input up to 26.3 kJ/kg  
29 then decreased dramatically at 58.2 kJ/kg. Longitudinal samples with shear work input <30  
30 kJ/kg, demonstrated significant strain hardening by all three estimation methods. At shear  
31 work inputs <30 kJ/kg, strong anisotropy was observed in both fracture stress and strain.  
32 After a shear work input of 58.2 kJ/kg, anisotropy and strain hardening were absent.  
33 Perpendicular samples did not show strain hardening at any level of shear work input.  
34 Although the distortion of the fat drops in the cheese structure associated with the elongation  
35 could account for some of the anisotropy observed, the presence of anisotropy in the  
36 elongated nonfat samples reflected that shear work and rolling also aligned the protein  
37 structure.

38 Key words: Tensile testing, Strain hardening, Anisotropy, Mozzarella cheese

39

## INTRODUCTION

40

41 Hot water stretching and kneading form an essential step in the traditional manufacture of  
42 Mozzarella cheese. This process step causes the proteins to flow giving a plastic appearance  
43 and forming a fibrous protein network aligned in the direction of stretching (McMahon et al.,  
44 1999). The fibrous structure is visible on a macroscopic level (Oberger et al., 1993; Sharma et  
45 al., 2016a). Sharma et al. (2016a, b; 2017) studied the effect of shear work input during this  
46 stretching and working step on the rheology and microstructure of model Mozzarella cheeses  
47 manufactured in a twin screw Blentech cooker at 70 °C. Shear work inputs were extended  
48 well beyond normal manufacturing limits to exaggerate any changes in the cheese caused by  
49 working. Mechanical properties were characterized using a range of rheological methods  
50 including steady shear viscosity, strain sweeps, frequency sweeps, temperature sweeps, and  
51 creep behavior. With increase in shear work input cheeses showed increases in steady shear  
52 viscosity and storage modulus. Frequency sweeps at 70 °C demonstrated a shift from  
53 viscoelastic liquid to viscoelastic solid. These changes all indicate work thickening of the  
54 cheese. Very high shear work inputs (>70 kJ/kg) led to major macroscopic structural changes  
55 to the cheese network with disappearance of the fibrous structure, loss of stretch and melt,  
56 and serum syneresis. Microstructures of the overworked cheeses indicated disappearance of  
57 the fibrous character and the creation of a homogeneous structure with a fine dispersion of fat  
58 particles in a brittle protein network (Sharma et al., 2017). The observed phenomena were  
59 attributed mainly to an increase in the strength of protein-protein interactions with prolonged  
60 working.

61 Bast et al. (2015) developed a tensile testing method to quantitate the anisotropy and strain  
62 hardening of commercial Mozzarella cheese. The method involved deliberate elongation of  
63 cheese at 60 °C by manual rolling on a cooled metal surface to ensure that the structure was

64 systematically aligned. Mozzarella cheeses showed strong anisotropy for both fracture stress  
65 and strain after elongation and also showed significant strain hardening in the longitudinal or  
66 fiber direction. The study indicated that tensile testing was a good method to explore  
67 anisotropy and strain hardening because fracture location and mode of failure were clearly  
68 visible. Other studies on strain hardening in dairy protein systems explored fine stranded  
69 whey protein isolate gels (Lowe et al., 2003), weak  $\beta$ -lactoglobulin gels (Pouzot et al., 2006)  
70 and gels formed by acidifying transglutaminase cross-linked casein (Rohm et al., 2014).

71 Rheological properties, microstructure and extent of anisotropy are all closely related to the  
72 functional characteristics of Mozzarella cheese for pizza application such as meltability,  
73 stretchability, elasticity, oiling-off and blister formation (Kindstedt and Fox, 1993; Olivares  
74 et al., 2009).

75 Strain hardening **behavior** expresses the underlying arrangement of structural units, is  
76 therefore useful for understanding functional properties of food materials. Strain hardening is  
77 well explored in gluten networks because it is important to attain optimum baking  
78 performance of bread dough by aiding holding capacity and stability of gas bubbles in the  
79 bread (Peighambardoust et al., 2006; Peressini et al., 2008; Kokelaar et al., 1996; Van Vliet et  
80 al., 1992; Van Vliet, 2008). The effect of mechanical work on tensile fracture properties and  
81 strain hardening of flour dough has also been studied. Peighambardoust et al. (2006) and  
82 Peressini et al. (2008) observed a decrease in strain hardening upon prolonged working of  
83 flour doughs and attributed this to breakdown in the gluten network structure. Structural  
84 analogy of anisotropic nature of gluten network and Mozzarella cheese indicates possibilities  
85 of adapting testing procedures from dough rheology for better understanding of strain  
86 hardening in Mozzarella type cheeses.

87 The objectives of this paper are: 1.To measure the tensile fracture properties and anisotropy  
88 of model Mozzarella cheeses with varied shear work inputs (3.3-73.7 kJ/kg) to complement  
89 the other rheological tools we have used; 2. To explore whether our model Mozzarella  
90 cheeses strain harden and to see the effect of shear work input on this strain hardening; and 3.  
91 To apply to Mozzarella cheese a wider range of strain hardening measures as used for flour  
92 doughs.

## 93 MATERIALS AND METHODS

### 94 *Materials*

95 Frozen blocks (-20 °C) of renneted, acidified protein gel prepared from skim milk were  
96 obtained from Fonterra Research and Development Centre (FRDC) pilot plant (Palmerston  
97 North, NZ). The protein gel was typically about 50% moisture and 46% protein. The frozen  
98 blocks were thawed for 1 d at 11 °C and ground to 6 mm grind size. Cream was obtained  
99 from FRDC as a fresh lot on each trial day. Cheese salt and tri-sodium citrate (TSC) were  
100 procured from Dominion Salt (Mount Maunganui, New Zealand) and Jungbunzlauer (Basel,  
101 Switzerland), respectively.

### 102 *Manufacture of model Mozzarella cheeses*

103 Model Mozzarella cheese was manufactured by mixing, cooking and working protein gel,  
104 cream, water and salt together using 150 rpm at 70 °C in a counter rotating twin-screw cooker  
105 (Blentech, model CC-0045, Blentech Corporation, Rohnert Park, CA, USA) (Sharma, et al.,  
106 2016a). Three model cheeses were prepared – full fat, nonfat and full fat with 0.5 % tri-  
107 sodium citrate (TSC) as a chelating agent. The target composition of full fat cheese was 23%  
108 fat, 21 % protein, 53% moisture and 1.4 % salt. The same protein to salt and protein to  
109 moisture ratios as in full fat cheese were used in nonfat cheese. Further details of processing

110 methods, sampling times, sample storage conditions and product compositions were given by  
111 Sharma et al. (2016a). Each experimental run was repeated twice on a different day at least  
112 one month interval in order to ensure that no variation arising from raw materials with similar  
113 composition but obtained from different lots.

114 All cheeses used in this study were frozen after manufacture. Shear work input was estimated  
115 by numerical integration of power-time curves (Sharma et al., 2016a). Shear work inputs  
116 ranged from 3.3 to 73.7 kJ/kg.

### 117 *Sample preparation for tensile testing*

118 Cheese samples were prepared for tensile testing using the method of Bast et al. (2015) with  
119 some variations. Cheese samples (~300 g) were melted by placing in closed container at 65  
120 °C water bath for about 2 h. Melted cheese was manually rolled on a cooled (4 °C) aluminum  
121 plate using a granite rolling pin (4 °C) to form a sheet. Aluminum guide strips were attached  
122 to the plate sides to achieve a sheet thickness of 3-4 mm. The term elongation is used  
123 throughout the paper for this process. Elongation was performed for 120 s at 10 rolls min<sup>-1</sup>.  
124 Dumbbell-shaped samples were cut in both longitudinal (n=8) and perpendicular (n=9)  
125 orientations. Samples were kept at 21 °C for at least 1 h before tensile testing. Each rolling  
126 treatment was performed twice.

### 127 *Tensile testing and data analysis*

128 Tensile testing on elongated cheese samples was performed on a TA.XT2plus Texture  
129 Analyzer (Stable Micro Systems Ltd., Godalming, UK) using tensile grips at 21 °C. Cross  
130 head speed was 2 mm s<sup>-1</sup> and trigger force was 0.01 N. The initial dimensions of the central  
131 section of each sample were measured using vernier calipers. Dumbbell-shaped samples were  
132 placed carefully on both jaws avoiding any fracture during sample transfer.

133 Force-displacement data were converted into true stress ( $\sigma$ , Pa) versus Hencky strain ( $\epsilon$ )  
134 (Bast et al., 2015). The anisotropy ratio, R, for fracture stress was calculated as  $\sigma_L/\sigma_P$  where  
135  $\sigma_L$  and  $\sigma_P$  are the fracture stresses in longitudinal and perpendicular directions, and similarly  
136 for fracture strain.

### 137 *Strain hardening parameters*

138 Strain hardening properties were calculated only for longitudinal samples as perpendicular  
139 samples showed no strain hardening. An empirical equation suggested by Hollomon  
140 (Kokelaar et al., 1996; van Vliet, 2008) provided two strain hardening parameters in uniaxial  
141 extension.

$$142 \quad \sigma = K_{SH} \epsilon_H^{n_{SH}} \quad (1)$$

143 where  $K_{SH}$  is the strength coefficient (Pa) and  $n_{SH}$  is strain hardening index (SHI). Values of  
144  $n_{SH} > 1$  indicate strain hardening behavior. Equation (1) was fitted ( $R^2 \sim 0.98-0.99$ ) to stress-  
145 strain data over the strain range 0.4 to “0.05 before fracture”.

146 Strain hardening is observed directly as an increase in the slope of the true stress-Hencky  
147 strain curve with increasing strain. A strain hardening ratio was therefore calculated (Bast et  
148 al., 2015)

$$149 \quad \text{Strain hardening ratio (SHR)} = \frac{\text{Maximum Modulus near fracture}}{\text{Initial modulus}} \quad (2)$$

150 Initial modulus was obtained by linear regression of each stress-strain curve in the strain  
151 range 0.01-0.25.

152 Strain hardening provides stability against uneven distribution of stress and incipient  
153 **localized** thinning allowing much larger extensions to occur, and allowing the material to  
154 resist further thinning by locally increasing the resistance to further deformation



155 (Dobraszczyk and Vincent, 1999). According to the Considère criterion for necking stability  
156 in uniaxial extension

$$157 \frac{d\sigma}{d\varepsilon} = \sigma \quad (3)$$

$$158 \text{ Apparent strain hardening (ASH)} = \frac{d \ln \sigma}{d\varepsilon} \quad (4)$$

159 ASH values  $> 1$  indicate strain hardening (van Vliet et al., 1992, van Vliet, 2008;  
160 Peighambardoust et al., 2006).

### 161 ***Microscopy***

162 Confocal scanning laser microscopy (CSLM) was done with a Zeiss LSM 510 META  
163 confocal microscope (Carl Zeiss AG, Oberkochen, Germany) according to the method of  
164 Sharma et al. (2017). Cheese slabs (~12 x 4 mm) were frozen at -20 °C and sectioned into 50  
165 µm slices on a cryo-microtome. Slices were immediately transferred to glass slides, stained  
166 with 0.4% Nile red and 0.2% fast green and covered with a coverslip. Samples were kept at 4  
167 °C for at least 48 h before imaging to allow uniform uptake of dyes.

168 Because nonfat cheese was translucent, microstructure could be studied using transmission  
169 light microscopy on an Olympus BX60 (Olympus Optical Co. Ltd, Tokyo, Japan). A 1 mm  
170 slice (12 x 12 mm) of nonfat cheese was prepared using a sharp razor blade. Images were  
171 captured by a CCD camera (Axio Cam HRc, Carl Zeiss, Hallbergmoos, Germany).

### 172 ***Rheological measurements***

173 Rheological measurements were conducted on an Anton Paar MCR 301 rheometer (Anton  
174 Paar, Graz, Austria) with a 20 mm diameter serrated plate geometry (PP20/P2) and a Peltier  
175 temperature hood (H-PTD 200) using the method of Sharma et al. (2015) for steady shear  
176 rheology and of Sharma et al. (2016b) for frequency sweeps. Disc shaped samples 20 mm

177 diameter and ~ 2-3 mm thick were cut using a cork borer and wire cutter. Cheese discs were  
178 held at 70 °C for 2 min to ensure isothermal conditions. The perimeter of cheese discs was  
179 covered with a ring of soybean oil to prevent moisture loss. Flow curves were obtained at 70  
180 °C using the method developed by Sharma et al. (2015) and a power law model fitted to the  
181 data to obtain consistency coefficient K and flow **behavior** index, n. Shear rates were applied  
182 with measurement times as follows: 60 s at 0.01 s<sup>-1</sup>, 6.25 s at 0.1 s<sup>-1</sup>, 0.5 s at 1 s<sup>-1</sup>, 0.05 s at 10  
183 s<sup>-1</sup>, 0.05 s at 100 s<sup>-1</sup>, 0.05 s at 200 s<sup>-1</sup>. Frequency sweeps applied frequencies in descending  
184 order at 20 °C. Rheological measurements were conducted in triplicate.

### 185 *Statistical analysis*

186 Descriptive statistics, non-linear regression and ANOVA analysis were conducted on the data  
187 using SPSS software (version 20). Significant differences (P < 0.05) in the results were  
188 **analyzed** using single factor ANOVA and the Duncan post hoc test to compare means.

## 189 **RESULTS**

### 190 *Tensile fracture properties of sheared model Mozzarella cheese*

191 Both longitudinal and perpendicular samples exhibited non-linear stress/strain behavior (Fig.  
192 1). At low strains ( $\epsilon < 0.25$ ) both longitudinal and perpendicular samples behaved in a linear  
193 manner with similar values of initial modulus. At small deformations, Hookean **behavior** is  
194 expected in food materials. However, at higher strain levels ( $\epsilon > 0.25$ ) nonlinear **behavior** was  
195 observed. Longitudinal samples demonstrated strain hardening with a significant increase in  
196 tensile modulus. Further measures to quantify strain hardening are explored in section 3.2.  
197 Perpendicular samples exhibited slight strain softening. Perpendicular samples fractured at  
198 much lower strain.

199 For full fat cheese, all longitudinal samples at shear work levels  $\leq 26.3$  kJ/kg produced  
200 similar stress-strain curves (Fig. 2a). At small strains ( $\varepsilon < 0.25$ ), initial modulus of  
201 longitudinal samples was about 129 kPa at shear work levels  $\leq 26.3$  kJ/kg but much higher  
202 (216 kPa) at 58.2 kJ/kg, indicating the creation of a stiffer structure upon working.  
203 Perpendicular samples (Fig. 2b) showed much more variation in stress-strain curves with  
204 reduction in fracture strain with increasing shear work input. Longitudinal and perpendicular  
205 samples indicated strain hardening and strain weakening behavior respectively. When a shear  
206 work of 58.2 kJ/kg was used to make the cheese, both longitudinal and perpendicular samples  
207 showed strain weakening behavior and had a low fracture strain. When comparing  
208 longitudinal samples of the 3 model cheeses (Fig. 2c), the order of both initial stiffness and  
209 extent of non-linear behavior was nonfat > full fat > TSC added cheese.

210 Longitudinal samples of full fat cheese indicated no significant difference in fracture stress,  
211 fracture strain or curve shape with shear work input up to 26.3 kJ/kg (Table 1), indicating  
212 similar structure and strength. However, there was a dramatic decrease in both fracture stress  
213 and strain at 58.2 kJ/kg. The decrease ( $P < 0.05$ ) in fracture stress with increase in shear work  
214 suggested that the cheese matrix had lower strength after prolonged working. Similar  
215 observations were made from tensile testing of dough systems subjected to different levels of  
216 working (Peighambardoust et al., 2006). The initial tensile modulus of the cheese increased  
217 dramatically from 142.1 kPa at 26.3 kJ/kg to 248.4 kPa at 58.2 kJ/kg (Table 2). Fracture  
218 stress did not change significantly with shear work input for perpendicular samples (Table 1),  
219 whereas fracture strain decreased significantly as shear work increased. Fracture strain is  
220 usually regarded as an indicator of structural arrangement, so decrease in fracture strain with  
221 increasing shear work indicates significant differences in structure, e.g. more inherent  
222 weaknesses in the structure causing crack initiation, propagation and fracture (Table 1, Fig.  
223 2b). The large percentage variations in fracture strain for perpendicular samples (Table 1)

224 probably arise from the random occurrence of such structural weaknesses or imperfections.  
225 At low shear work inputs of 3.3-26.3 kJ/kg for the full fat cheeses, longitudinal samples had  
226 higher values for both fracture stress ( $\sigma_f = 115-128$  kPa) and fracture strain ( $\epsilon_f = 0.74-0.77$ )  
227 than the perpendicular samples ( $\sigma_f = 27-40$  kPa;  $\epsilon_f = 0.29-0.37$ ). Anisotropy index was higher  
228 for fracture stress (3.0-4.5) than for fracture strain (2.0-2.6). Both indicated significant  
229 anisotropy ( $P < 0.05$ ) in fracture properties. At a shear work input of 58.2 kJ/kg, anisotropy  
230 had disappeared for both fracture stress and fracture strain (Table 1).

231 Fracture stress for nonfat cheese was ~33 % higher ( $P < 0.05$ ) for longitudinal samples and  
232 ~59 % higher ( $P < 0.05$ ) for perpendicular samples than that for full fat cheese with similar  
233 shear work input (Table 1). Nonfat cheese had a much higher protein content than full fat  
234 cheese, so more structural protein elements were present per unit cross-sectional area in the  
235 nonfat cheese giving rise to higher values of fracture stress. Adding TSC to full fat cheese  
236 resulted in ~32% lower ( $P < 0.05$ ) fracture stress than full fat cheese for both longitudinal and  
237 perpendicular samples. This may be attributed to chelation of calcium by added TSC,  
238 resulting in loose binding of cheese matrix (Sharma et al., 2016a).

239 The different cheeses behaved very differently during the elongation process (Fig. 3) and this  
240 had an impact on their tensile fracture **behavior**. At low and moderate shear work inputs, the  
241 cheese elongated well giving a smooth, homogeneous cheese layer (Fig. 3a). At 58.2 kJ/kg  
242 shear work, the cheese did not flow well giving a heterogeneous cheese layer with a number  
243 of weak spots (Fig. 3b). With excessive working (73.7 kJ/kg), rolling could not be  
244 conducted satisfactorily as even at 65 °C the cheese was brittle, there was no continuous  
245 flowing mass and the resulting cheese sheet was highly heterogeneous (Fig. 3c).  
246 Representative dumbbell tensile samples could not be cut from the cheese sheet.

247 ***Strain hardening of model Mozzarella cheeses***

248 Strain hardening parameters for samples cut in longitudinal orientation are presented in Table  
249 2. SHI was the least variable parameter (coefficient of variation ~4%) followed by ASH  
250 (~7%) and then SHR (~13%). The SHR method was the most variable and is the ratio of two  
251 moduli. In contrast, ASH,  $K_H$  and SHI were estimated from fits to the whole non-linear  
252 portion of the fracture curve and were probably a better indicator of strain hardening. For the  
253 full fat cheeses with shear work input up to 26.3 kJ/kg SHR varied from 1.65 to 1.81, ASH  
254 from 2.51 to 2.60 and SHI from 1.30 to 1.33. For all 3 parameters values greater than 1  
255 indicate strain hardening (Bast et al., 2015 for SHR; Peighambardoust et al., 2006 for ASH;  
256 van Vliet et al., 1992, van Vliet, 2008 for SHI), so strain hardening is significant. In contrast,  
257 at a shear work input of 58.2 kJ/kg, strain softening was observed with both SHR (0.76) and  
258 SHI (0.49) being less than 1. Decreased ( $P<0.05$ ) strain hardening with an increase in shear  
259 work input from 26.3 kJ/kg to 58.2 kJ/kg suggested weakening of the cheese matrix or a  
260 higher prevalence of fracture initiating cracks with progressive working. Peighambardoust et  
261 al. (2006) also reported a reduction in ASH values with progressive mixing of bread dough.  
262 Zheng et al. (2000), Gras et al. (2000) and Peressini et al. (2008) concluded that over-mixing  
263 led to diminished tensile fracture properties of bread dough under extension tests.

264 The nonfat cheese and TSC added cheese samples also showed significant strain hardening  
265 for all 3 parameters (Table 2). The ASH and SHI values were significantly higher ( $P<0.05$ )  
266 for nonfat cheese (2.84 and 1.35) and lower ( $P<0.05$ ) for TSC added cheese (2.39 and 1.25)  
267 than for full fat cheese (2.57 and 1.32) with similar shear work input (Table 2). Table 2 also  
268 presents results for fracture tests performed on nonfat cheese at constant strain rate rather  
269 than constant crosshead speed. The TA.XT2plus was programmed to increase crosshead  
270 speed with time in order to maintain a constant strain rate of  $0.2 \text{ s}^{-1}$ . This indicated an even  
271 higher extent of strain hardening with ASH and SHI both significantly higher (3.55 and 1.42)  
272 than at constant crosshead speed (2.84 and 1.35).

### 273 ***Structural anisotropy in model cheeses***

274 Cheeses before elongation exhibited microstructural anisotropy with orientation of fat in one  
275 direction (Fig. 4a1, a2). Tensile testing of these unrolled cheeses during preliminary studies,  
276 however, showed no significant anisotropy for either fracture stress or fracture strain. After  
277 melting and elongation the same cheeses still revealed signs of microstructural anisotropy  
278 with the fat channels enlarged (Fig. 4b1, b2, b3). The structure showed globular fat in some  
279 regions (Fig. 4b3) and coalesced, elongated fat particles in other regions (Fig. 4b2). This  
280 microstructural alignment of fat particles was presumably a major contributor to anisotropy in  
281 tensile fracture properties. Nonfat cheese samples also indicated microstructural alignment of  
282 the protein structure by transmission light microscopy (Fig. 4c). A simple photograph of  
283 nonfat cheese macrostructure also suggested orientation in the direction of rolling (Fig. 3d).  
284 Similar structural orientation has been reported previously at various length scales for nonfat  
285 cheeses (Mizuno and Lucey, 2005) supporting our observations.

### 286 ***Small strain oscillatory shear rheology of model cheeses***

287 Mechanical spectra at 20 °C of full fat, nonfat and TSC added cheeses are shown in Fig. 5.  
288 All three cheeses exhibited viscoelastic solid behavior ( $G' > G''$  across all frequencies tested)  
289 with low and similar frequency dependence (slope,  $n_f \sim 0.16 - 0.18$ ), suggesting the presence  
290 of a physically stable network. The  $n_f$  values are consistent with those reported for casein gels  
291 and fat-filled casein gels (Zhou and Mulvaney, 1998). Storage moduli for full fat cheese were  
292 higher than those for nonfat cheese and TSC added cheese, probably because of the  
293 contribution from solid fat at 20 °C (Zhou and Mulvaney, 1998). The storage modulus of  
294 milkfat ( $G_f' = 292$  kPa) was higher than that of the cheese matrix ( $G_m' = 164$  kPa) at 20 °C  
295 (Yang et al., 2011), so fat would be expected to reinforce the matrix.

### 296 ***Steady shear rheology of elongated model cheeses***

297 Bast et al. (2015) noted that the manual rolling process caused considerable work thickening  
298 in as little as 18 s, whereas shear in the Blentech caused almost no work thickening after 4000  
299 s at 50 rpm (Sharma et al., 2016a). It is interesting to know whether the work thickening from  
300 elongation was only evident in tensile fracture properties or whether it also caused changes in  
301 steady shear viscosity. Consistency coefficient and apparent viscosity at  $0.01 \text{ s}^{-1}$  increased by  
302 1.43 and 1.52 times respectively ( $P < 0.05$ ) after elongation (Table 3). This indicates  
303 significant work thickening upon elongation. Elongation also increased tensile fracture stress  
304 by 5.7 times parallel to the fibers and by 2.1 times perpendicular to the fibers (Bast et al.,  
305 2015). The type of deformation is quite different in measurement of the two properties  
306 though. Tensile fracture measures the strength of a material while pulling in one direction  
307 whereas steady shear rheology measures resistance to shear flow.

## 308 DISCUSSION

309 The anisotropy index range for fracture stress of 3.01-4.49 (Table 1) for our elongated model  
310 cheeses was similar to the value for an elongated commercial Mozzarella cheese (3.0) but  
311 less than that for string cheese (6.0) (Bast et al., 2015) or fibrous fat-calcium caseinate  
312 materials (highest 14.2) (Manski et al., 2008). Possible reasons for the higher degree of  
313 anisotropy in other reports were the higher protein to moisture ratio for string cheese (0.59  
314 compared to 0.39), the presence of transglutaminase cross-linking enzyme in the material of  
315 Manski et al. (2008) and the use of specific shearing processes that increased the fibrous  
316 character in both the examples quoted.

317 To help explain anisotropy in full fat, elongated model Mozzarella cheese, we propose a  
318 structural model (Fig. 6a). The proposed model is based upon assumption that fracture  
319 process uses viscolastic mode of energy release in isothermal conditions. A continuous  
320 protein-gel contains a dispersed phase of fat particles elongated in the direction of rolling as

321 observed by CSLM (Fig. 4b). At small strains ( $<0.25$ ), the stress-strain curves for  
322 longitudinal and perpendicular samples are very similar because the main deformation is in  
323 the gel network, e.g. initial modulus 126 kPa for longitudinal and 116 kPa for perpendicular  
324 samples (Fig. 1). As strain increased perpendicular to the long axis of the fat particles,  
325 fracture was initiated at low strains because of the large amount of structurally weak fat and  
326 fat-protein interface in this orientation. This resulted in lower values of fracture stress and  
327 strain for the perpendicular orientation (Table 1). As strain increased parallel to the long axis  
328 of the fat particles, fracture **occurred** in the gel phase as there was much less fat-protein  
329 interface. Fracture was reached at higher strains and therefore higher fracture stress. The  
330 anisotropy of cooked meat has been explained in a similar way with the muscle fibers having  
331 higher strength than the connective tissue between the fibers (Purslow, 1985).

332 Nonfat cheese was also highly anisotropic (Table 1) and showed evidence of structural  
333 alignment at a macroscopic/visual scale (Fig. 3d) and a microscopic scale (Fig. 4c). Structural  
334 alignment at a microscopic scale was also observed by Mizuno and Lucey (2005). Nonfat  
335 mozzarella cheese has been shown to contain serum pockets (Paulson et al., 1998; Pastorino  
336 et al., 2002; McMahon et al., 2005). These pockets would be aligned in the direction of  
337 rolling forming weak interfaces between the protein fibers as depicted in Fig. 6a. An  
338 alternative explanation is that shearing in the Blentech or elongation by rolling may be  
339 causing **localized** fracture or shear banding as observed in dough systems (Kieffer and Stein,  
340 1999, Peighambardoust et al., 2006), resulting in reduced bond strength between fractured  
341 planes. Shear banded gluten structures led to a fibrous texture and were regarded as a major  
342 cause for structural anisotropy in sheared dough (Peighambardoust et al., 2006). Strain  
343 exerted in the perpendicular orientation may cause early fracture because of weak bonding  
344 between fibers (Taneya et al, 1992; Ak and Gunasekaran, 1997), while strain in the  
345 longitudinal orientation requires fracture of the fibers resulting in higher fracture strains and



346 stresses. This explanation for nonfat cheese anisotropy must be combined with that in the  
347 paragraph above to get a more complete picture for full fat cheese, i.e. alignment of the  
348 protein structure is an important factor in explaining the anisotropy of full fat cheese. The  
349 observed changes and distortions of the fat phase were probably an indicator of related  
350 microstructural changes occurring in the protein phase.

351 Strain hardening in flour dough has been more widely studied (e.g. Kokelaar et al., 1996; van  
352 Vliet et al., 1992; van Vliet, 2008; Peighambardoust et al., 2006 and Peressini et al., 2008)  
353 than strain hardening of protein structures based on casein. Peighambardoust et al. (2006)  
354 reported that flour doughs strain hardened perpendicular to the fibers as well as parallel and  
355 that fracture strain was often higher for perpendicular samples than for longitudinal samples.  
356 Fracture stress usually showed no anisotropy apart from dough from one type of flour  
357 (Spring). The results of Manski et al. (2008) using sheared and transglutaminase cross-linked  
358 casein structures are more similar to ours in that strong anisotropy was observed and only  
359 longitudinal samples strain hardened, not perpendicular samples. A possible model to explain  
360 strain hardening suggests two casein structural elements - individual polymer molecules and  
361 elongated clusters of cross-linked casein polymers (Fig. 6b). Crosslinked elements are  
362 assumed to be stiffer. After strain hardening, three major changes are depicted – both  
363 elements are more aligned, the initial cross-links are more tightly bound and additional cross-  
364 linking has occurred. Zhang et al., (2007) proposed calcium induced junction zones as a  
365 possible reason for strain hardening **behavior** in alginate gels. The crosslinks depicted in Fig.  
366 6b would have a similar role to these junction zones in causing strain hardening and calcium  
367 is again likely to be involved.

368 The loss of both strain hardening and anisotropy of full fat cheese at high shear work input  
369 (58 kJ/kg) derives from changes in the microscopic structure of the material. The presence of

370 fat and serum channels in Mozzarella-type cheeses is widely reported (Paulson et al., 1998;  
371 McMahon et al., 1999; Mizuno and Lucey, 2005; McMahon et al., 2005). Sharma et al.  
372 (2017) presented CSLM images of striated protein structures with aligned fat-serum channels  
373 at moderate shear work levels (3.3-25.3 kJ/kg) in model Mozzarella cheeses and attributed  
374 this to the laminar mixing action in the Blentech. These striated structures lead to mechanical  
375 and structural anisotropy in fat-protein networks at various length scales (Cervantes et al.,  
376 1983; Ak and Gunasekaran, 1997; Manski et al., 2008; Bast et al., 2015; Sharma et al., 2015).  
377 At high shear work inputs (>58 kJ/kg) the striated structure had disappeared and a  
378 macroscopically homogenous, isotropic cheese structure occurred with finely dispersed fat  
379 and no fibrous nature or stretch (Sharma et al., 2016a, 2017). This cheese showed no  
380 structural or mechanical anisotropy. Parallel behavior was reported for prolonged working of  
381 flour dough in a z-blade mixer (Peighambaroust et al., 2006). Decreases in tensile fracture  
382 stress, fracture strain and ASH were observed with progressive mixing, indicating weakening  
383 of the dough matrix. Strain hardening in flour dough depends on the amount and quality of  
384 gluten so the loss of ASH was attributed to extensive breakdown of the gluten network  
385 structures.

386 The higher values of fracture stress for nonfat cheese compared to full fat cheese are because  
387 the fat particles act as weak areas in the structure. Bast et al. (2015) demonstrated that the  
388 tensile strength of milkfat at 21 °C was very low. It is interesting that the strain hardening  
389 parameters for nonfat cheese were mostly not significantly different from those for full fat  
390 cheese in spite of the higher protein content and the absence of low strength fat in the  
391 structure. The addition of a calcium chelating salt (TSC) to the cheese was expected to result  
392 in reduced but still flexible interactions between proteins in the structure, leading to a weaker  
393 but still cohesive structure (Sharma et al., 2016a). Fracture stress for TSC added cheese (78.5  
394 kPa) was much lower ( $P < 0.05$ ) than full fat cheese (115.7 kPa) and nonfat cheese (159.2 kPa)

395 (Table 1) as expected but fracture strain was not significantly different. It is interesting that  
396 TSC addition reduced work thickening in the Blentech to a very low level (Sharma et al.,  
397 2016a) but did not reduce strain hardening very much (Table 2). Cheese with TSC added still  
398 strain hardens as observed by all three measures used. The role of calcium in the strain  
399 hardening bonding mechanism appears to be less important as compare with the work  
400 thickening bonding mechanism. It would be interesting to look at the effect of extent of  
401 chelation of calcium in detail on rheological and fracture properties of cheese.

402 Steady shear viscosity increased by 52% after simple elongation of model Mozzarella cheese  
403 for 120 s whereas shearing in the Blentech at 50 rpm for 4000 s caused only small increases  
404 in steady shear viscosity (Sharma et al., 2016a). The one dimensional elongational flow  
405 caused by rolling with simultaneous cooling into the more elastic region was apparently very  
406 effective at work thickening. One possible explanation of the results is that rolling causes  
407 elongation of the primary protein particles thus increasing viscosity because the particles with  
408 a higher aspect ratio occupy more hydrodynamic volume. On the other hand, remelting of  
409 elongated cheese leads to relaxation of structure and decrease in anisotropy with some loss of  
410 strength (Bast et al., 2015).

411 One aspect of the results that is not well understood is that although the structure is  
412 macroscopically fibrous and the microstructure shows anisotropy there is no anisotropy in the  
413 stress-strain curves at strains below about 0.25 (Fig. 1). The anisotropy only develops at  
414 higher strains and is largely related to the fact that longitudinal samples strain harden at  
415 strains  $> 0.25$ , whereas perpendicular samples begin to strain weaken and then fracture.  
416 Based on the previous discussion by Bast et al. (2015), we suggest one possible mechanism.  
417 In the initial or linear region on the stress-strain curve, strain is merely straightening curves or  
418 bends in the protein network, which may be the same in the two orientations. In the

419 exponential or strain hardening region, where straightening has reached its limit, the fibers in  
420 the longitudinal direction need to be stretched or move past one another, leading to strain  
421 hardening. In the perpendicular orientation the fibers are pulled further apart, the interfaces  
422 are weak and maybe there are also more microcracks for initiation of fracture. This plausible  
423 mechanism will require further experimental evidence for validation.

424

## CONCLUSIONS

425 Both strain hardening and anisotropy were observed after elongation in sheared model  
426 Mozzarella cheeses at moderate levels of shear work (3.3-26.3 kJ/kg). Structural alignments  
427 of both protein and fat phases were regarded as major contributing factors to this behavior.  
428 Strain hardening and anisotropic character were absent from a model cheese with prolonged  
429 working (>58 kJ/kg) because the structure was homogeneous and isotropic but also contained  
430 a number of weak spots. Anisotropy and strain hardening were also observed with nonfat  
431 cheese. We attribute this to the presence of macroscopic protein fibers in the direction of  
432 rolling even in the absence of fat. Schematic models are proposed to explain strain hardening  
433 and anisotropy in a full fat model Mozzarella cheese. The model consists of fat dispersed in a  
434 gel matrix having two structural elements, cross-linked and non-cross-linked caseins.

435

## ACKNOWLEDGEMENTS

436 The authors are grateful to Fonterra Co-operative Group and the Ministry for Primary  
437 Industries for funding this project via the Transforming the Dairy Value Chain Primary  
438 Growth Partnership programme in Food Structure Design. We thank Robbie Buwalda,  
439 Bhavin Parmar, Ben Somerton, Grant Bleakin, Dave Griffin and Ken Anderson for their help  
440 with the Blentech trials at FRDC. We thank Elizabeth Nickless and Michael Loh, FRDC for  
441 helping with confocal laser scanning microscopy and light microscopy analysis of cheese  
442 samples.

443

## REFERENCES

444 Ak, M. M., and S. Gunasekaran. 1997. Anisotropy in tensile properties of mozzarella cheese.

445 J. Food Sci. 62:1031-1033. <http://dx.doi.org/10.1111/j.1365-2621.1997.tb15031.x>.

446 Bast, R., P. Sharma, H. K. B. Easton, T. T. Dessev, M. Lad, and P.A. Munro. 2015. Tensile

447 testing to quantitate the anisotropy and strain hardening of Mozzarella cheese. Int. Dairy J.

448 44: 6-14. <http://dx.doi.org/10.1016/j.idairyj.2014.12.006>.

449 Cervantes, M. A., D. B. Lund, and N. F. Olson. 1983. Effects of salt concentration and

450 freezing on Mozzarella cheese texture. J. Dairy Sci. 66:204-213.

451 [http://dx.doi.org/10.3168/jds.s0022-0302\(83\)81778-0](http://dx.doi.org/10.3168/jds.s0022-0302(83)81778-0).

452 Dobraszczyk, B. J. and J. F. V. Vincent. 1999. Measurement of mechanical properties of food

453 materials in relation to texture: The material approach. Pages 99-151 in Food texture:

454 measurement and perception. A.J. Rosenthal, Ed., Aspen Publishers, Maryland, USA.

455 Gras, P. W., H. C. Carpenter and R. S. Anderssen. 2000. Modelling the developmental

456 rheology of wheat-flour dough using extension tests. J. Cereal Sci. 31:1-13.

457 <http://dx.doi.org/10.1006/jcrs.1999.0293>

458 Kieffer, R. and N. Stein. 1999. Demixing in wheat doughs—its influence on dough and

459 gluten rheology. Cereal Chem. 76:688-693. <http://dx.doi.org/10.1094/cchem.1999.76.5.688>

460 Kindstedt, P.S. and P.F. Fox. 1993. Effect of manufacturing factors, composition, and

461 proteolysis on the functional characteristics of mozzarella cheese. Crit. Rev. Food Sci. Nutr.,

462 3:167-187. <http://dx.doi.org/10.1080/10408399309527618>

463 Kokelaar, J.J., T. van Vliet, and A. Prins. 1996. Strain hardening properties and extensibility  
464 of flour and gluten doughs in relation to breadmaking performance. *J. Cereal Sci.* 24:199-  
465 214. <http://dx.doi.org/10.1006/jcrs.1996.0053>

466 Lowe, L.L., E. A. Foegeding, and C. R. Daubert. 2003. Rheological properties of fine-  
467 stranded whey protein isolate gels. *Food Hydrocoll.*17:515-522.  
468 [http://dx.doi.org/10.1016/s0268-005x\(03\)00014-6](http://dx.doi.org/10.1016/s0268-005x(03)00014-6)

469 Manski, J.M., E. E. J. van der Zalm, A. J. van der Goot, and R.M. Boom. 2008. Influence of  
470 process parameters on formation of fibrous materials from dense calcium caseinate  
471 dispersions and fat. *Food Hydrocoll.* 22:587-600.  
472 <http://dx.doi.org/10.1016/j.foodhyd.2007.02.006>.

473 McMahon, D. J., B. Paulson, and C. J. Oberg. 2005. Influence of calcium, pH, and moisture  
474 on protein matrix structure and functionality in direct-acidified nonfat Mozzarella cheese. *J.*  
475 *Dairy Sci.* 88:3754-3763. [http://dx.doi.org/10.3168/jds.s0022-0302\(05\)73061-7](http://dx.doi.org/10.3168/jds.s0022-0302(05)73061-7).

476 McMahon, D. J., R. L. Fife, and C. J. Oberg. 1999. Water partitioning in Mozzarella cheese  
477 and its relationship to cheese meltability. *J. Dairy Sci.* 82:1361–1369.  
478 [http://dx.doi.org/10.3168/jds.s0022-0302\(99\)75361-0](http://dx.doi.org/10.3168/jds.s0022-0302(99)75361-0).

479 Mizuno, R., and J. A. Lucey. 2005. Effects of emulsifying salts on the turbidity and calcium-  
480 phosphate-protein interactions in casein micelles. *J. Dairy Sci.* 88:3070–3078.  
481 [http://dx.doi.org/10.3168/jds.s0022-0302\(05\)72988-x](http://dx.doi.org/10.3168/jds.s0022-0302(05)72988-x)

482 Oberg, C. J., W. R. McManus, and D. J. McMahon. 1993. Microstructure of Mozzarella  
483 cheese during manufacture. *Food Struct.* 12:251-258.

484 Olivares, M.L., S.E. Zorrilla, and A.C. Rubiolo. 2009. Rheological properties of mozzarella  
485 cheese determined by creep/recovery tests: effect of sampling direction, test temperature and

486 ripening time. *J. Texture Stud.* 40:300-318. <http://dx.doi.org/10.1111/j.1745->  
487 [4603.2009.00183.x](http://dx.doi.org/10.1111/j.1745-4603.2009.00183.x).

488 Pastorino, A. J., R. I. Dave, C. J. Oberg, and D. J. McMahon. 2002. Temperature effect on  
489 structure-opacity relationships of nonfat Mozzarella cheese. *J. Dairy Sci.* 85:2106–2113.  
490 [http://dx.doi.org/10.3168/jds.s0022-0302\(02\)74288-4](http://dx.doi.org/10.3168/jds.s0022-0302(02)74288-4)

491 Paulson, B. M., D. J. McMahon, and C. J. Oberg. 1998. Influence of sodium chloride on  
492 appearance, functionality, and protein arrangements in nonfat Mozzarella cheese. *J. Dairy*  
493 *Sci.* 81:2053–2064. [http://dx.doi.org/10.3168/jds.s0022-0302\(98\)75780-7](http://dx.doi.org/10.3168/jds.s0022-0302(98)75780-7).

494 Peighambardoust, S.H., A.J. van der Goot, T. van Vliet, R.J. Hamer, and R.M. Boom, (2006).  
495 Microstructure formation and rheological behaviour of dough under simple shear flow. *J.*  
496 *Cereal Sci.* 43:183-197. <http://dx.doi.org/10.1016/j.jcs.2005.10.004>

497 Peressini, D., S. H. Peighambardoust, R. J. Hamer, A. Sensidoni, and A. J. van der Goot.  
498 2008. Effect of shear rate on microstructure and rheological properties of sheared wheat  
499 dough. *J. Cereal Sci.* 48:426-438. <http://dx.doi.org/10.1016/j.jcs.2007.10.008>

500 Pouzot, M., T. Nicolai, L. Benyahia, and D. Durand. 2006. Strain hardening and fracture of  
501 heat-set fractal globular protein gels. *J. Colloid Interface Sci.* 293:376-383.  
502 <http://dx.doi.org/10.1016/j.jcis.2005.06.074>

503 Purslow, P.P. (1985). The physical basis of meat texture: Observations on the fracture  
504 behaviour of cooked bovine M-semitendinosus. *Meat Sci.* 12:39-60.  
505 [http://dx.doi.org/10.1016/0309-1740\(85\)90024-5](http://dx.doi.org/10.1016/0309-1740(85)90024-5)

506 Rohm, H., F. Ullrich, C. Schmidt, J. Lobner, and D. Jaros. 2014. Gelation of cross-linked  
507 casein under small and large shear strain. *J. Texture Stud.* 45:130-137.  
508 <http://dx.doi.org/10.1111/jtxs.12056>

509 Sharma, P., T. T. Dessev, P. A. Munro, P. G. Wiles, G. Gillies, M. Golding, B. James, and P.  
510 Janssen. 2015. Measurement techniques for steady shear viscosity of Mozzarella-type cheeses  
511 at high shear rates and high temperature. *Int. Dairy J.* 47:102-108.  
512 <http://dx.doi.org/10.1016/j.idairyj.2015.03.005>.

513 Sharma, P., P. A. Munro, T.T. Dessev, and P.G. Wiles. 2016b. Shear work induced changes  
514 in the viscoelastic properties of model Mozzarella cheese. *Int. Dairy J.* 56:108-118.  
515 <http://dx.doi.org/10.1016/j.idairyj.2016.01.010>.

516 Sharma, P., P. A. Munro, T.T. Dessev, P.G. Wiles, and R.J. Buwalda. 2016a. Effect of shear  
517 work input on steady shear rheology and melt functionality of model Mozzarella cheeses.  
518 *Food Hydrocoll.* 54:266-277. <http://dx.doi.org/10.1016/j.foodhyd.2015.10.009>.

519 Sharma, P., P.A.Munro, G. Gillies, T.T. Dessev, and P.G. Wiles. 2017. Changes in creep  
520 behavior and microstructure of model Mozzarella cheese during working. *Lebenson. Wiss.*  
521 *Technol.* 83:184–192. <https://doi.org/10.1016/j.lwt.2017.05.003>

522 Taneya, S., T. Izutsu, T. Kimura, and T. Shioya, 1992. Structure and rheology of string  
523 cheese. *Food Struct.*11:61-71.

524 Van Vliet, T. 2008. Strain hardening as an indicator of bread-making performance: A review  
525 with discussion. *J. Cereal Sci.* 48:1-9. <http://dx.doi.org/10.1016/j.jcs.2007.08.010>

526 Van Vliet, T., A.M. Janssen, A.H. Bloksma, and P. Walstra. 1992. Strain hardening of dough  
527 as a requirement for gas retention. *J. Texture Stud.* 23:439-460.  
528 <http://dx.doi.org/10.1111/j.1745-4603.1992.tb00033.x>

529 Yang, X., N. R. Rogers, T. K. Berry, and E. A. Foegeding. 2011. Modeling the rheological  
530 properties of cheddar cheese with different fat contents at various temperatures. *J. Texture*  
531 *Stud.* 42:331-348. <http://dx.doi.org/10.1111/j.1745-4603.2011.00283.x>



532 Zhang, J., C.R. Daubert, and E.A. Foegeding. 2007. A proposed strain-hardening mechanism  
533 for alginate gels. *J. Food Eng.* 80:157-165. <http://dx.doi.org/10.1016/j.jfoodeng.2006.04.057>

534 Zheng, H., M. P. Morgenstern, O. H. Campanella, and N. G. Larsen. 2000. Rheological  
535 properties of dough during mechanical dough development. *J. Cereal Sci.* 32:293-306.  
536 <http://dx.doi.org/10.1006/jcrs.2000.0339>

537 Zhou, N., and S. J. Mulvaney. 1998. The effect of milk fat, the ratio of casein to water, and  
538 temperature on the viscoelastic properties of rennet casein gels. *J. Dairy Sci.* 81:2561-2571.  
539 [http://dx.doi.org/10.3168/jds.s0022-0302\(98\)75813-8](http://dx.doi.org/10.3168/jds.s0022-0302(98)75813-8)

540

**Table 1.** Effects of shear work on tensile fracture properties of model Mozzarella cheeses.

	Shear work kJ/kg	Fracture stress (kPa)			Fracture strain (-)		
		Longitudinal	Perpendicular	Anisotropy Ratio	Longitudinal	Perpendicular	Anisotropy Ratio
Full fat cheese	3.3	121.02 ± 26.97 <sup>a</sup>	40.24 ± 14.51 <sup>bc</sup>	3.01	0.75 ± 0.07 <sup>ac</sup>	0.37 ± 0.09 <sup>d</sup>	2.04
	4.3	115.72 ± 22.14 <sup>a</sup>	32.25 ± 12.07 <sup>bf</sup>	3.59	0.75 ± 0.09 <sup>a</sup>	0.34 ± 0.10 <sup>de</sup>	2.23
	8.8	125.45 ± 16.40 <sup>a</sup>	27.94 ± 8.18 <sup>bf</sup>	4.49	0.74 ± 0.06 <sup>ac</sup>	0.29 ± 0.09 <sup>e</sup>	2.54
	26.3	128.61 ± 21.50 <sup>a</sup>	30.60 ± 12.20 <sup>bf</sup>	4.20	0.77 ± 0.07 <sup>a</sup>	0.30 ± 0.09 <sup>e</sup>	2.58
	58.2	44.36 ± 14.55 <sup>bc</sup>	41.33 ± 11.20 <sup>bc</sup>	1.07	0.21 ± 0.05 <sup>b</sup>	0.22 ± 0.06 <sup>b</sup>	0.94
Nonfat cheese	6.8	159.24 ± 33.53 <sup>c</sup>	47.74 ± 17.65 <sup>e</sup>	3.34	0.68 ± 0.14 <sup>c</sup>	0.34 ± 0.07 <sup>de</sup>	2.03
Nonfat cheese – constant strain rate	6.8	140.77 ± 42.76 <sup>c</sup>	40.08 ± 8.06 <sup>e</sup>	3.5	0.58 ± 0.10 <sup>c</sup>	0.31 ± 0.05 <sup>de</sup>	1.87
TSC added full fat cheese	4.4	78.50 ± 19.24 <sup>d</sup>	21.92 ± 3.88 <sup>f</sup>	3.58	0.70 ± 0.09 <sup>ac</sup>	0.29 ± 0.04 <sup>e</sup>	2.45

Values are means with standard deviations from n=16 longitudinal samples and n=18 perpendicular samples (n=4 for constant strain rate experiment). Means for the same parameter, e.g. fracture stress, with different superscript letters are significantly different (P<0.05).

**Table 2.** Effect of shear work on strain hardening properties of model Mozzarella cheeses.

Sample	Shear work input (kJ/kg)	Initial modulus (kPa)	Maximum modulus (kPa)	Strain hardening ratio	Apparent strain hardening, $d\ln\sigma/d\varepsilon_H$	Strength coefficient, $K_H$ (Pa)	Strain hardening index, $n_H$
Full fat cheese	3.3	129.31 ± 10.05 <sup>a</sup>	235.48 ± 42.25 <sup>a</sup>	1.81 ± 0.24 <sup>a</sup>	2.60 ± 0.15 <sup>a</sup>	184.91 ± 20.89 <sup>ab</sup>	1.33 ± 0.05 <sup>a</sup>
	4.3	128.70 ± 17.74 <sup>a</sup>	219.73 ± 34.26 <sup>a</sup>	1.79 ± 0.26 <sup>a</sup>	2.57 ± 0.16 <sup>a</sup>	171.78 ± 29.36 <sup>ab</sup>	1.32 ± 0.05 <sup>a</sup>
	8.8	141.89 ± 14.77 <sup>a</sup>	231.46 ± 28.29 <sup>a</sup>	1.65 ± 0.27 <sup>a</sup>	2.52 ± 0.13 <sup>a</sup>	189.53 ± 13.16 <sup>b</sup>	1.30 ± 0.05 <sup>a</sup>
	26.3	142.13 ± 21.05 <sup>a</sup>	238.74 ± 40.92 <sup>a</sup>	1.72 ± 0.28 <sup>a</sup>	2.51 ± 0.10 <sup>a</sup>	181.20 ± 22.30 <sup>ab</sup>	1.31 ± 0.05 <sup>a</sup>
	58.2	248.44 ± 59.74 <sup>b</sup>	188.87 ± 48.07 <sup>b</sup>	0.76 ± 0.07 <sup>b</sup>	-	3.63 ± 1.31 <sup>c</sup>	0.49 ± 0.03 <sup>b</sup>
Nonfat cheese	6.8	174.01 ± 27.91 <sup>c</sup>	313.96 ± 58.86 <sup>c</sup>	1.76 ± 0.37 <sup>a</sup>	2.84 ± 0.09 <sup>b</sup>	273.52 ± 38.73 <sup>d</sup>	1.35 ± 0.08 <sup>a</sup>
Nonfat cheese - constant strain rate	6.8	198.14 ± 13.39 <sup>c</sup>	334.16 ± 9.25 <sup>c</sup>	2.03 ± 0.59 <sup>a</sup>	3.55 ± 0.20 <sup>d</sup>	366.97 ± 6.74 <sup>f</sup>	1.42 ± 0.01 <sup>d</sup>
TSC added full fat cheese	4.4	104.93 ± 5.97 <sup>d</sup>	148.30 ± 27.01 <sup>d</sup>	1.41 ± 0.23 <sup>c</sup>	2.39 ± 0.09 <sup>c</sup>	125.11 ± 14.47 <sup>e</sup>	1.25 ± 0.07 <sup>c</sup>

Values are means with standard deviations from n=16 longitudinal samples (n=4 for constant strain rate experiment). Means within a column with different superscript letters are significantly different (P<0.05).

**Table 3.** Effect of rolling on steady shear rheology of model Mozzarella cheese\* at 70°C

	Normal cheese	Rolled cheese
Consistency coefficient, K (Pa.s <sup>n</sup> )	131.2 ± 10.2 <sup>a</sup>	188.2 ± 20.2 <sup>b</sup>
Flow behaviour index, n	0.73 ± 0.01 <sup>a</sup>	0.72 ± 0.01 <sup>b</sup>
Apparent viscosity at 0.01 s <sup>-1</sup> , Pa.s	449.3 ± 8.3 <sup>a</sup>	682.7 ± 76.3 <sup>b</sup>

\* Cheese was prepared by giving 26.3 kJ/kg of shear work input at 150 rpm and 70 °C

Values are means with standard deviations from 4 repetitions. Means within a row with different superscript letters are significantly different (P<0.05)

Sharma Fig 1.

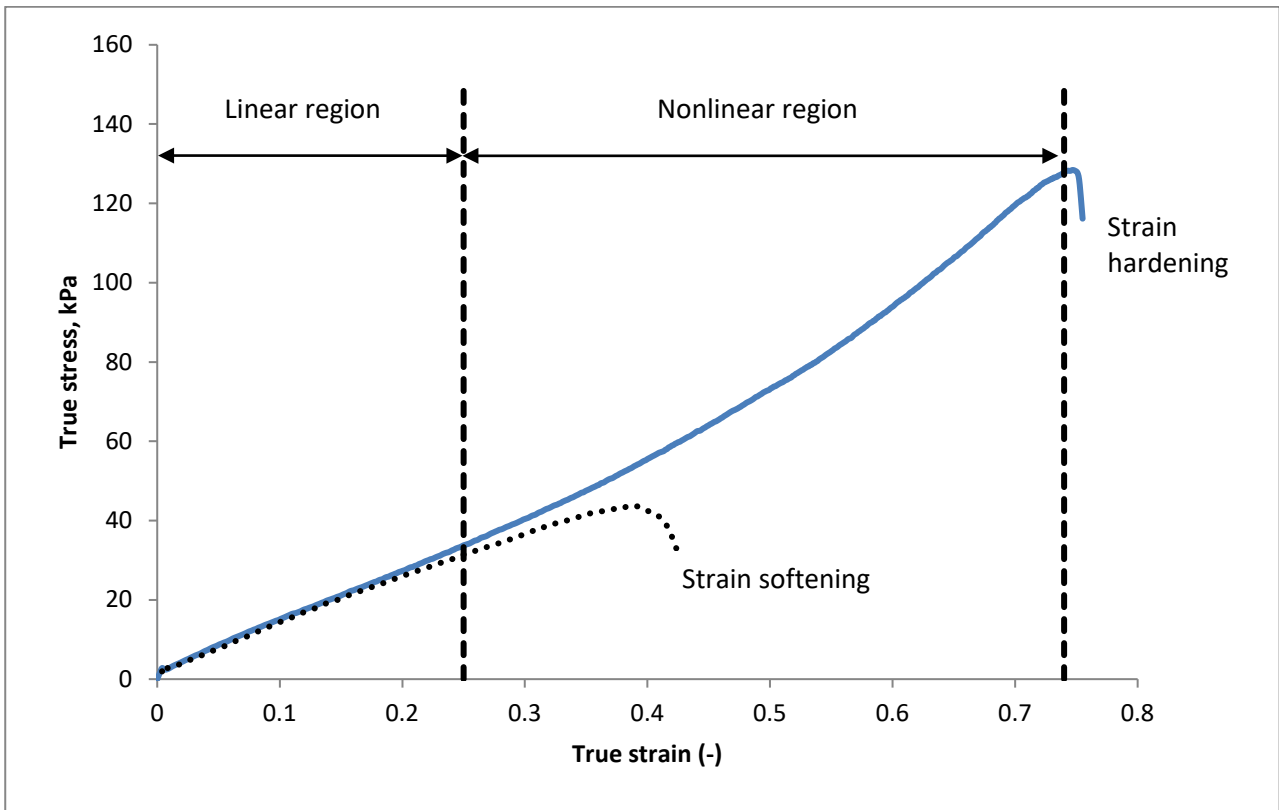


**Fig. 1.** Typical stress-strain curves for model Mozzarella cheese samples in longitudinal (smooth line) and perpendicular (dotted line) orientations indicating strain hardening and strain softening respectively. Longitudinal samples show linear and nonlinear regions before tensile fracture. Model Mozzarella cheeses were prepared in the Blentech cooker with 3.3 kJ/kg of shear work at 70 °C using 150 rpm screw speed.

Sharma Fig. 2

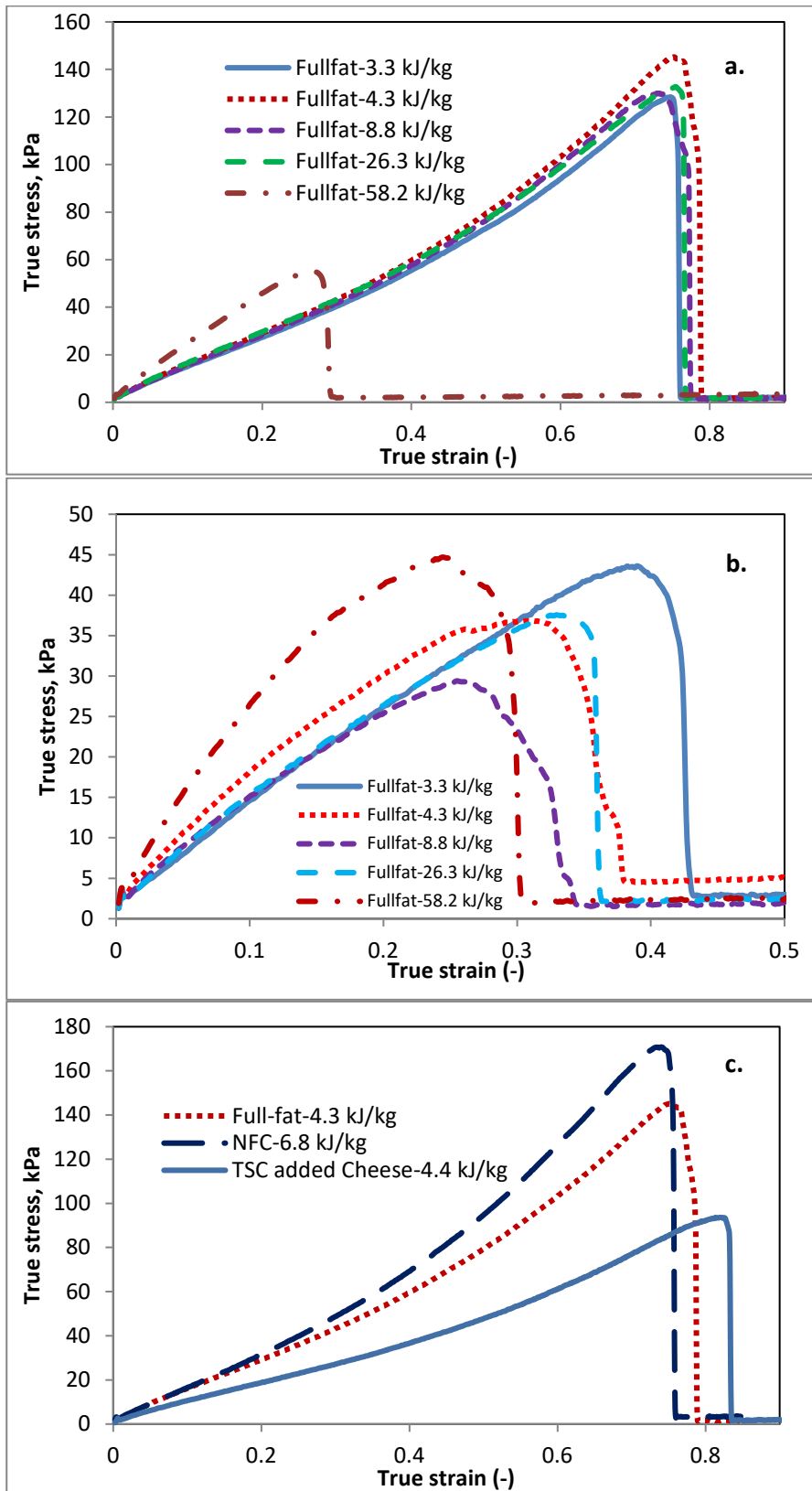


**Fig. 2.** Stress-strain curves for model Mozzarella cheeses. Cheeses with varied amounts of shear work were cut in both longitudinal (a) and perpendicular (b) orientations. Full fat, nonfat and TSC added cheeses are compared at a similar shear work level in longitudinal orientation (c). Model Mozzarella cheeses were prepared in the Blentech cooker at 70 °C using 150 rpm screw speed. Typical curves close to the mean behaviour were chosen from n=16 longitudinal samples and n=18 perpendicular samples.



Sharma Fig. 3

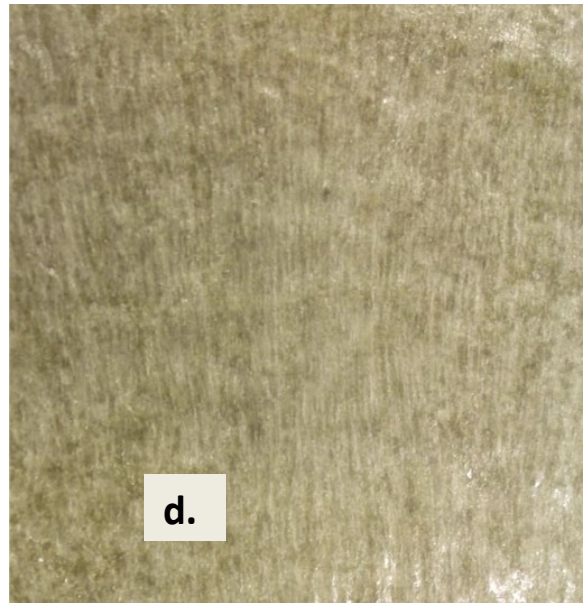
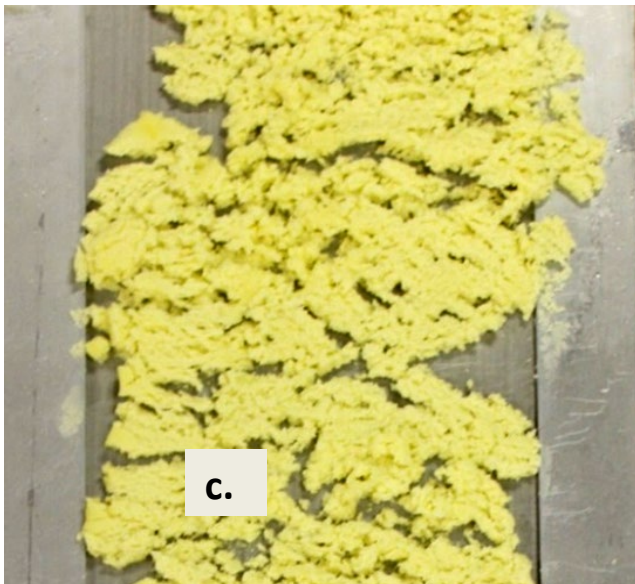
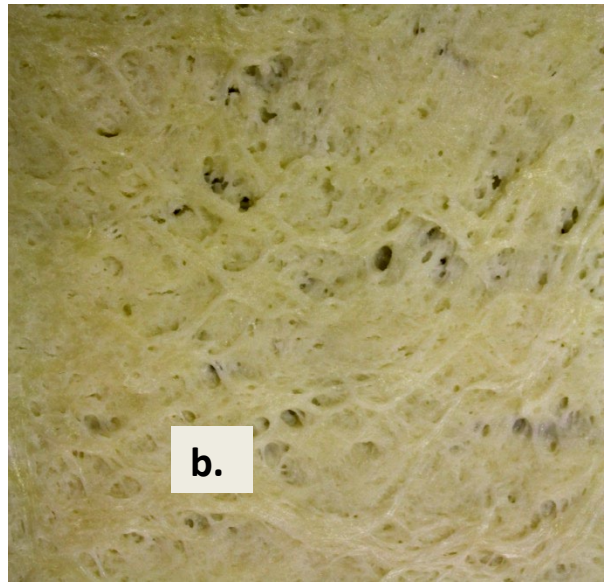


**Fig. 3.** Visual appearance of elongated model Mozzarella cheeses. Cheese samples were prepared in the Blentech cooker with varied amounts of shear work input at 70 °C and 150 rpm; full fat cheese a. 8.8, b. 58.2, c. 73.7 kJ/kg, nonfat cheese d. 6.8 kJ/kg

Sharma Fig. 4

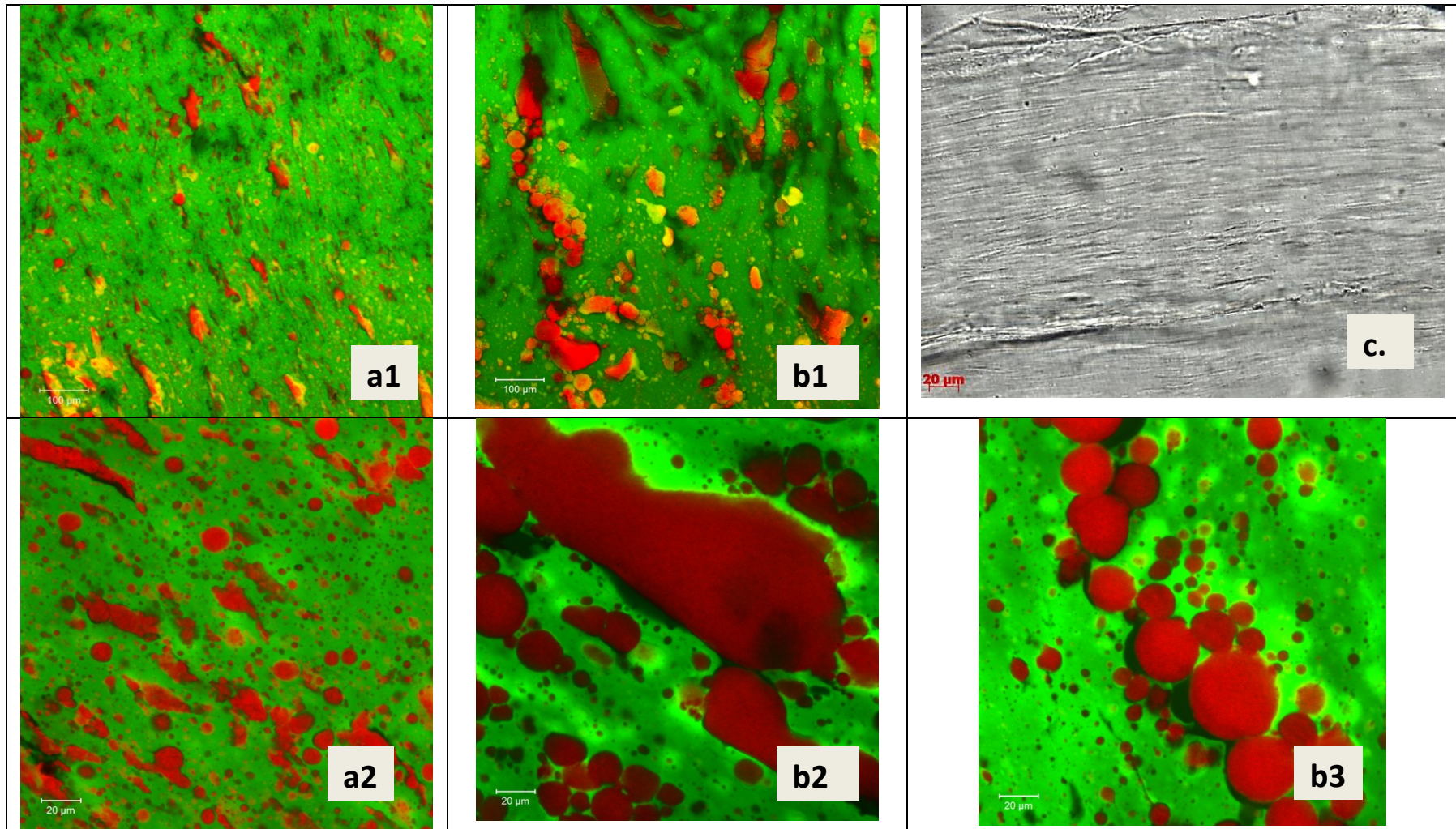


**Fig. 4.** Microstructures of model Mozzarella cheeses; CSLM images of normal (a1,a2) and elongated (b1,b2,b3) full fat Mozzarella cheeses after 26.3 kJ/kg of shear work input; Light microscopy (LM) image of nonfat Mozzarella cheese (c) after 6.8 kJ/kg of shear work input. Cheese samples were prepared in the Blentech cooker at 70 °C and 150 rpm. Red - fat, green - protein and black - air/water.

Sharma Fig. 5

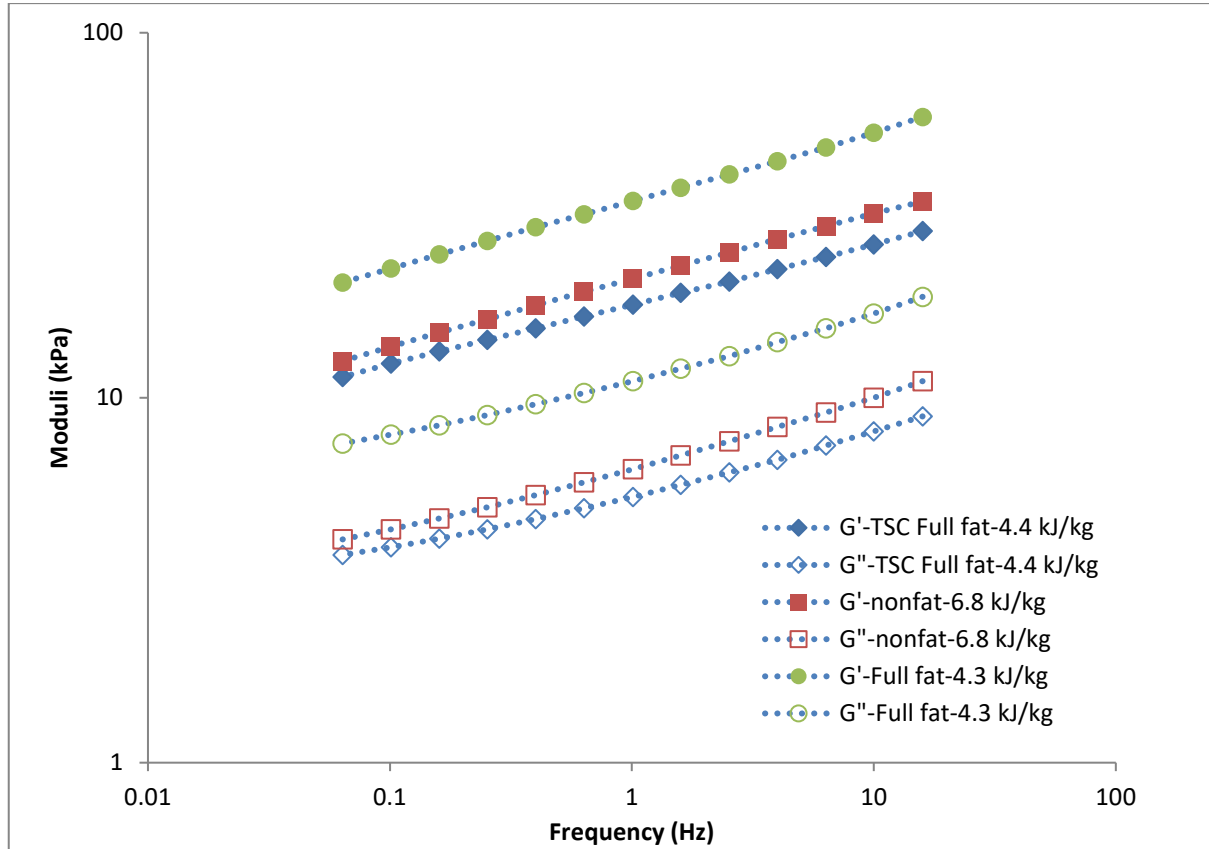


**Fig. 5.** Storage moduli (closed symbols) and loss moduli (open symbols) of model Mozzarella cheeses obtained from frequency sweeps at 20 °C on full fat, nonfat and TSC added cheeses by giving 4.3, 6.8 and 4.4 kJ/kg of shear work input respectively at 70 °C and 150 rpm.



Sharma Fig. 6

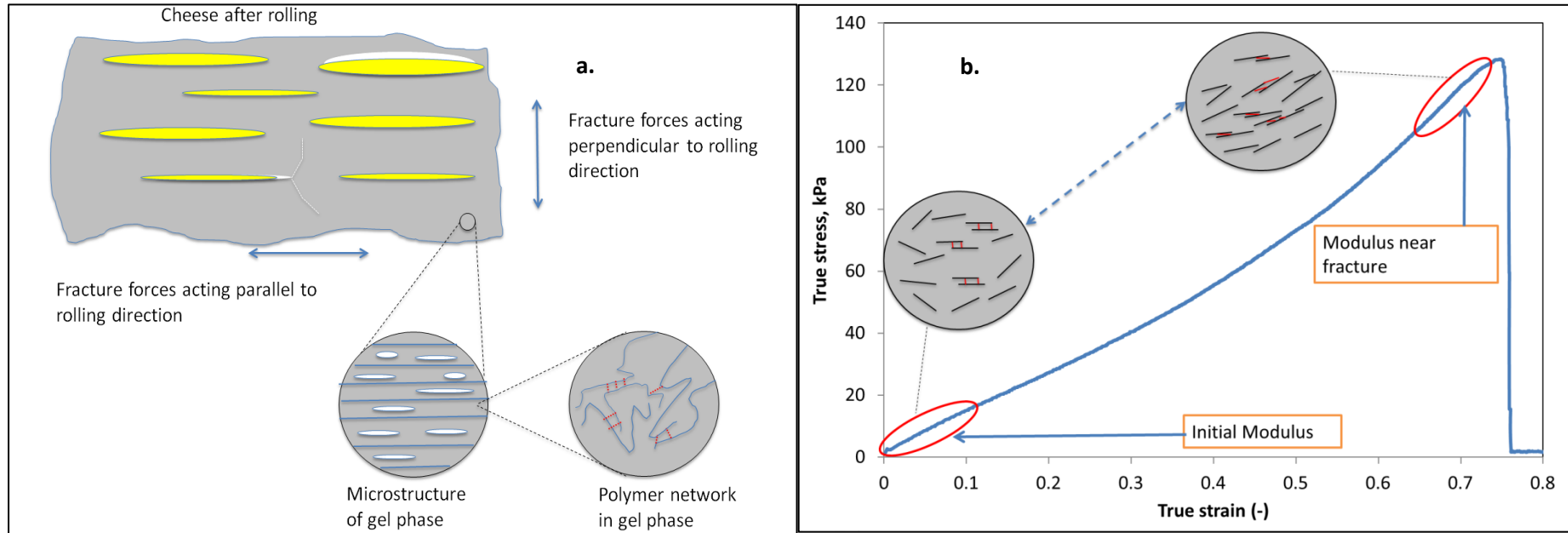


**Fig. 6.** Schematic model explaining structural basis for anisotropy (a) and strain hardening (b) during tensile fracture of Model Mozzarella cheeses. Grey and yellow areas indicate gel phase and fat phase respectively. White pockets in gel phase indicate serum/water portion. Further structural elements within the gel phase are presented in magnified grey circles.